

Double nuclear spin relaxation in hybrid quantum Hall systemsM. H. Fauzi,^{1,2,*} William J. Munro,^{4,3} Kae Nemoto,^{3,†} and Y. Hirayama^{1,5,6,‡}¹*Center for Spintronics Research Network, Tohoku University, Sendai 980-8577, Japan*²*Research Center for Physics, National Research and Innovation Agency, South Tangerang City, Banten 15314, Indonesia*³*National Institute of Informatics, 2-1-2 Hitotsubashi, Chiyoda-ku, Tokyo 101-8430, Japan*⁴*NTT Basic Research Laboratories & NTT Research Center for Theoretical Quantum Physics, NTT Corporation, 3-1 Morinosato-Wakamiya, Atsugi-shi, Kanagawa, 243-0198, Japan*⁵*Department of Physics, Tohoku University, Sendai 980-8578, Japan*⁶*Center for Science and Innovation in Spintronics (Core Research Cluster), Tohoku University, Sendai 980-8577, Japan*

(Received 30 August 2020; revised 31 August 2021; accepted 2 September 2021; published 10 September 2021)

Recent advances in quantum engineering have given us the ability to design hybrid systems with novel properties normally not present in the regime they operate in. The coupling of spin ensembles and magnons to microwave resonators has for instance lead to a much richer understanding of collective effects in these systems and their potential quantum applications. We can also hybridize electron and nuclear spin ensembles together in the solid-state regime to investigate collective effects normally only observed in the atomic, molecular, and optical world. Here we explore in the solid state regime the dynamics of a double domain nuclear spin ensemble coupled to the Nambu-Goldstone boson in GaAs semiconductors and show it exhibits both collective and individual relaxation (thermalization) on very different time scales. Further the collective relaxation of the nuclear spin ensemble is what one would expect from superradiant decay. This opens up the possibility for the exploration of novel collective behavior in solid state systems where the natural energies associated with those spins are much less than the thermal energy.

DOI: [10.1103/PhysRevB.104.L121402](https://doi.org/10.1103/PhysRevB.104.L121402)

It has now be widely accepted that the principles of quantum mechanics will lead to new technologies with capabilities unlike anything seen in our purely classical world [1–3]. There is the potential to have computational and communication power beyond anything our conventional world can every realize [4–6]. The principles also allow us to construct unparalleled quantum sensing and imaging sensitivity [7,8]. Typically such achievements could be achieved using traditional quantum systems. However, in recent years, it has been established that the hybridization of distinct quantum systems has the potential to design composite devices with properties and attributes not normally unavailable in the regime those systems came from [9–11]. Hybrid quantum systems will exhibit functionalities superior to those in other sub quantum systems and are likely to be multitasking [11]. They will play important roles in engineering multi-functional quantum devices and performing diverse quantum information processing tasks. With the state-of-the-art quantum technology, hybrid quantum systems are being designed and engineered using many different types of elements ranging from solids to atomic, molecular and optical (AMO) systems [9–18].

Hybrid quantum systems are more however than a tool to create new technologies as they also provide the opportunity to explore quantum many body and nonequilibrium

physics in unique regimes or regimes normally not available to those systems [11,20,21]. We now have the ability to explore quantum phenomena using solid-state systems which have typically been investigated in AMO systems [20–24] with the advantage that this solid-state systems are easier to control, manipulate and measure with high accuracy. Two recent examples include the demonstration of amplitude bistability and superradiance using an electronic spin ensemble coupled to a microwave resonator [20,21]. The latter case is of particular interest here as it involves the collective behavior of that ensemble where the superradiant burst of microwave photons occurred ten orders of magnitude faster than the corresponding relaxation of a single nitrogen-vacancy center in diamonds electron spin [21]. While this was a coherence phenomena, a simple modification using two ensembles instead of one allows it to be a truly collective quantum phenomena with no classical analog [25,26]. It also raises the question about whether such collective effects can be seen in other solid-state systems which we will explore in this context. Further by using nuclear spins, one would be operating in a regime with significant thermal background, even though the experiment is taking place in a dilution environment [27–29].

The predication and subsequent demonstration of the quantum Hall (QH) effect establishing macroscopic quantum phenomena in solid-state two-dimensional electron systems in the presence of high magnetic field has spawned many important discoveries in quantum many-body electronic physics and topological quantum matter including the quantum Hall ferromagnet and collective excitations such as Nambu-Goldstone

*moha065@lipi.go.id

†nemoto@nii.ac.jp

‡yoshiro.hirayama.d6@tohoku.ac.jp

(NG) bosons and skyrmions [30–34]. However, the nuclear-electron spin dynamics and its hybridization in the QH system has been rarely explored [35]. Coupling of a nuclear spin ensemble to a Nambu-Goldstone boson seems an ideal candidate to explore collective effects in a solid-state hybrid quantum system [25,34] and that would be our focus here. We would expect to observe phenomena arising from both collective and individual nuclear spins decoherence and so our initial focus will be on the measured behavior of this hybrid system - especially the dynamic ones. A Nambu-Goldstone mode is known to cause a rapid nuclear spin relaxation rate [34,36,37]. However, the way that the nuclear spin dynamics was measured in the previous reports missed out a key feature, which we address here namely a sudden reconfiguration of nuclear spin polarization.

Our hybrid quantum system as depicted in Fig. 1(a) is implemented in a GaAs-based bilayer quantum Hall setting [38]. We bring the electronic state into the quantum Hall regime where the interplay between charge, spin, and layer degree of freedom creates nontrivial correlated electronic states [39,40]. For our situation here, the initialization of our double nuclear-spin domains with different spin orientation (\uparrow and \downarrow) is achieved by electrical means using a fractional quantum Hall liquid (FQHL) [41] developed at the bottom layer, where $2/3$ of the available states in the lowest Landau level are occupied [42]. It exhibits two different magnetic phases, spin polarized and unpolarized phases, which are separated by a domain wall at the spin transition point [43]. Now the injection of a relatively large alternating source-drain current I_{sd} at the spin transition point creates a bidirectional nuclear spin polarization due to multiple forward scattering events between two neighboring magnetic phases [44,45]. As a result the double-nuclear-spin domain is generated with a state of the form $|\text{DNSD}\rangle = |\uparrow \dots \uparrow\rangle_A \otimes |\downarrow \dots \downarrow\rangle_B$ where the first domain (labelled A) has all spins pointed up \uparrow while the second domain B has all spins pointed down \downarrow . We expect the domain to have approximately the same number of nuclear spins in them but a little asymmetry could exist [46].

Our initial state $|\text{DNSD}\rangle$ is illustrated in Fig. 2(a) where we vary the pumping time τ_p to observe its effect on the magnetization of each domain. Here the blue (red) dots represent the degree of nuclear spin polarization of the up (down)-spin domain which are measured in terms of a change in the hyperfine field. The degree of spin polarization (resulting from the dynamical spin flip-flop process between the electron and nuclear spins driven by the source-drain current I_{sd}) in each domain increases with larger pumping time τ_p reaching a maximum of 6.6% (4.0%) respectively. Without such pumping the thermal equilibrium polarization is much less than 1%.

Having described one half of our hybrid system, let us now describe the second system which is a NG boson. The NG boson arises from a charge imbalance in the QH state of the bilayers at total filling factor $\nu_{\text{tot}} = 2$ as depicted in Fig. 1(b). We can tune this charge imbalance δn to realize three different spin phases/configurations: The canted antiferromagnetic (CAF) phase, the ferromagnetic (FM) phase and the spin-singlet (SS) phase [34,40,47]. The charge imbalance changes the strength of the tunneling gap (Δ_{SAS}) relative to the electronic Zeeman energy (E_Z), thereby allowing us to access those three different phases at will. It is the CAF phase that

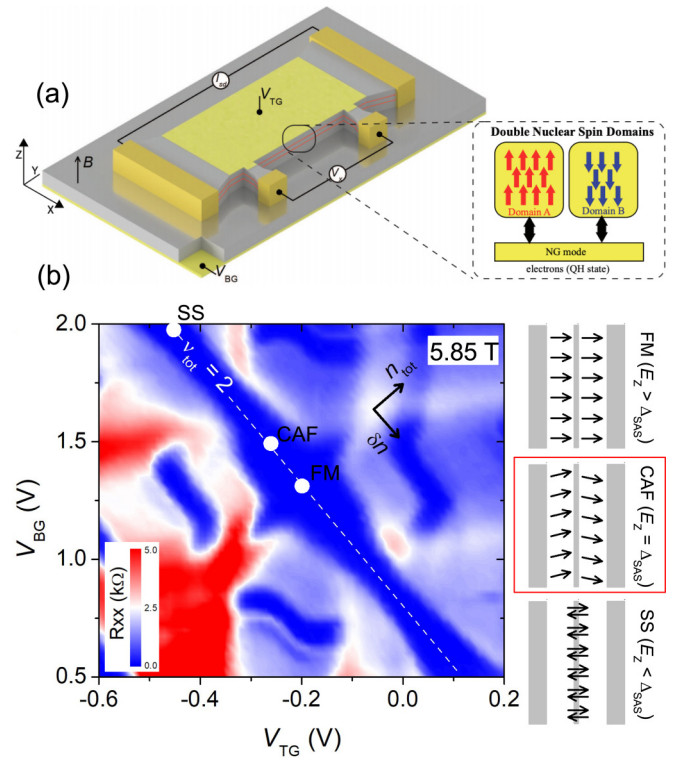


FIG. 1. (a) Schematic illustration of our hybrid quantum systems device used to investigate the behavior of nuclear spins coupled with an electronic reservoir of electrons in QH states through the hyperfine interaction. Here two identical 20-nm wide GaAs quantum wells, indicated by the two red lines, are in close proximity to create a strongly coupled bilayer two-dimensional electron gas system. The electronic states in both layers are electrostatically controlled by applying a gate bias between the top gate (V_{TG}) and bottom gate (V_{BG}). The inset depicts our QH system coupled through the hyperfine interaction to the NG boson. The nuclear spins are forming the double-spin domains A and B (two independent ensembles) with the NG boson operating as a reservoir. Domain A is described by the upward red arrows while domain B with the downward blue arrows. The number of spins in each domain is approximately the same. (b) A color map of longitudinal resistance as a function of top and bottom gate measured at a field of 5.85 T and a lattice temperature of 50 mK. We highlight the data around total filling factor $\nu_{\text{tot}} = 2$ where three different electron spin configurations (FM, CAF, and SS) along the dotted white line can be realized depending on the charge imbalance (δn) between the two layers. Among those three possible spin states at $\nu_{\text{tot}} = 2$, the CAF phase houses the NG boson mode.

is of interest here as it supports a linear dispersing NG boson in the long-wavelength limit [39]. The NG boson naturally couples with the double-nuclear-spin polarized domains [48] allowing us to create our required hybrid system [49]. To set the electronic state to the CAF phase, we set the top (bottom) gate bias to $V_{TG} = -0.23$ V ($V_{BG} = +1.5$ V), respectively.

In Fig. 2(b), we show the effect of coupling our double domain system to the NG boson for a given pumping time before measuring the total magnetization of the system (which indicates the degree of polarization of the hybrid system). It is clear that this coupling has rapidly increased the degree of polarization in the system as shown by the black dotted

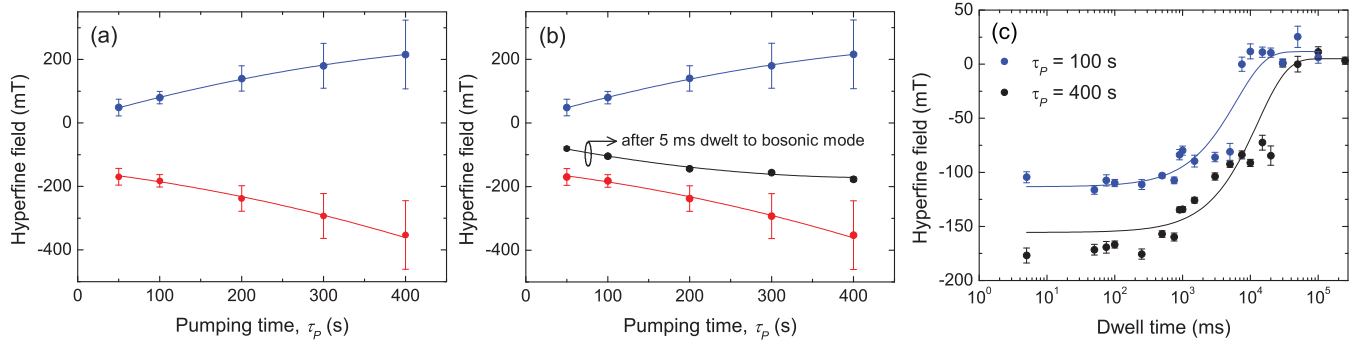


FIG. 2. Plot of the initialization of the double-nuclear-spin domain (a) indicating the number of polarized nuclear spins (measured as a hyperfine field change in millitesla) vs the time τ_p the source-drain current I_{sd} is applied. At $\tau_p = 50$ s, the number of up nuclear spin polarization J_{\uparrow}^z (down nuclear spin polarization J_{\downarrow}^z) was -170 mT ($+43$ mT), respectively. For $\tau_p = 400$ s, they increased to -353 mT ($+215$ mT), a factor of 2 (5) polarization improvement, respectively. As a calibration a fully polarized sample would result in a hyperfine field near 5.3 T [19] meaning we can estimate the maximum percentage of spins in the up (down) domain at approximately 6.6% (4%) respectively. In (b), we depict the total nuclear spin polarization for varying pumping time τ_p followed by a 5-ms interaction the NG boson with a subsequent total magnetization measurement (in terms of the hyperfine field strength). For ease of comparison, the initial polarization in (a) is replotted. In (c), we show the nuclear spin relaxation dynamics vs the Dwell time to the NG boson for pumping times $\tau_p = 100$ s (400 s) respectively with the solid lines providing a visual guide. It is clear that at long times the double-nuclear-spin domains reach the same thermal equilibrium. Our minimum dwell time measurement is 5 ms restricting our ability to explore the really short time dynamics.

curve—actually to a magnetization below that associated with thermal equilibrium. This leads to the natural question about what our system is doing and so let us now explore the dynamics of this system. We let the double nuclear spin system and NG boson interact for a given dwell time before we measure the polarization of the entire double domain system using a simple magnetization measurement. We clearly observe [as shown in Fig. 2(c)] that the nuclear spins from the double domain system has relaxed very rapidly (<5 ms) and are pointing upwards (parallel to the direction of the applied magnetic field). They stay in the relaxed state until around 1 s where it begins to thermalize to its original thermal steady state. The rethermalization is completed near 100 s. A sudden reconfiguration of nuclear spin polarization and its dynamics towards equilibrium are completely different from an ordinarily independent relaxation process.

It is apparent from Fig. 2(c) that our hybrid system has a number of interesting and independent timescales associated with it. Two of these are associated with the usual dephasing [19,50] and thermalization processes with timescales given by $T_2^* \sim 1$ ms and $T_1 \sim 40$ s, respectively [51]. These correspond clearly to the behavior seen in the right-hand side of that sub-figure. The left-hand side of the figure with the flat region in between 5 and 500 ms is however much more interesting and only occurs because of the coupling to the NG boson associated with the CAF phase. The FM and SS phases do not show this short term behavior. This is due to the fact that they have gapped modes [48] meaning the double nuclear spins exhibit normal relaxation processes independent of the initial number of polarized nuclear spins [52] (see Supplemental Material). It is thus clear our observed behavior here is associated with the canted antiferromagnetic (CAF) phase and its associated NG boson. It is critical to determine how this relaxation caused by the coupling to the NG boson varies with the size of the total nuclear spin ensemble. We have already established in Fig. 2(a) that the hyperfine field strength (proportional to the number of polarized nuclear spins in the

ensemble) increases with increasing pumping time τ_p . Thus we can prepare different size nuclear spin polarized ensembles which we can then let interact with the NG boson for 5ms before measuring the resulting polarization. In Fig. 2(b), we plot the total spin polarization (measured by the hyperfine field) against the pumping time τ_p after its interaction with the NG boson.

We clearly observe that the nuclear spin polarization of the total double domain system increasing as the pumping time τ_p gets larger. It is clear from Figs. 2(b) and 2(c) that this short time behavior is associated with the form of the NG boson coupling to the double nuclear spin domain. As such we need to explore this in a little more detail.

When we tune the two-dimensional QH state such that the in-plane rotational symmetry of electron spin is spontaneously broken, an associated linear dispersing NG boson emerges. This can be described by a continuous wave-number vector $\mathbf{k} = (k_x, k_y)$ with wavelength ~ 0.1 nm for a nuclear-spin frequency near 10 MHz. This long wavelength is very important as the nuclear-spin separation is approximately ~ 0.5 nm (much shorter than that of the NG boson) meaning those nuclear spins can couple collectively to the NG boson. This is our first hint at a collective effect where the NG boson is acting like a reservoir [48]. It also gives us a natural way to model our overall hybrid system. For simplicity, we assume that all the spins here are identical (only single species to be taken into account) with spin 1/2.

Our hybrid quantum system composed of two nuclear spin ensembles and the NG boson can be effectively described by the Dicke model where the NG boson act as a reservoir [48]. This model indicates the generation of collective phenomena of nuclear spins. In actual systems, however, there are individual dissipative effects which break the collective phenomena. Examples include a dipole-dipole interaction between nuclear spins which induces a dephasing effect and an individual coupling between spin and other reservoir like phonon leading to a T_1 -time relaxation process. Given the presence of collective

effect involving a quantum/thermal reservoir as well as individual nuclear spin dephasing and thermalization, it is quite natural to model this system by a nuclear spin Born-Markov type master equation [53] of the form

$$\begin{aligned} \dot{\rho}(t) = & -i\omega_{\text{ns}}[J_A^z + J_B^z, \rho(t)] \\ & + \frac{\gamma^{\text{rel}}}{2} [(\bar{n} + 1)\mathcal{L}([J_A^- + J_B^-]\rho) + \bar{n}\mathcal{L}([J_A^+ + J_B^+]\rho)] \\ & + \frac{\gamma^{\text{rel}}}{2} \left[(\bar{n} + 1) \sum_{i_{A,B}=1}^{N_{A,B}} \mathcal{L}(I_{i_{A,B}}^- \rho) + \bar{n} \sum_{i_{A,B}=1}^{N_{A,B}} \mathcal{L}(I_{i_{A,B}}^+ \rho) \right] \\ & + \frac{\gamma^{\text{dep}}}{2} \left[\sum_{i_A=1}^{N_A} \mathcal{L}(I_{i_A}^z \rho) + \sum_{i_B=1}^{N_B} \mathcal{L}(I_{i_B}^z \rho) \right], \quad (1) \end{aligned}$$

where $J_{A,B}^z = \sum_{i_{A,B}=1}^{N_{A,B}} I_{i_{A,B}}^z$ are the collective spin Z-operators for the domain A (B) with $I_{i_{A,B}}^z$ representing the individual nuclear spin 1/2 z operator. Here $N_{A,B}$ are the total number of spins included in the domain A and B, respectively (the combined number of spins in both ensembles is $N = N_A + N_B$). Associated with these are the collective (individual) raising $J_{A,B}^+$ ($I_{i_{A,B}}^+$) and lowering $J_{A,B}^-$ ($I_{i_{A,B}}^-$) operators for the nuclear spins in domain A and B, respectively. The nuclear spin frequency is given by $\omega_{\text{ns}} = \gamma_n B$ where γ_n being the gyromagnetic ratio of nuclear spins. Further γ^{rel} (γ^{dep}) in our master equation represent the damping (dephasing) rates. Next $\bar{n} = 1/(e^{\hbar\omega_{\text{ns}}/k_B T} - 1)$ is the Bose-Einstein distribution functions at the energy $\hbar\omega_{\text{ns}}$ for a given temperature T where k_B is the Boltzmann constant. In (1), the Liouvillian $\mathcal{L}(X\rho)$ is given by $\mathcal{L}(X\rho) = 2X\rho X^\dagger - X^\dagger X\rho - \rho X^\dagger X$ with X being an arbitrary operator.

Our master equation given by (1) describes four basic phenomena; the Larmor precession of nuclear spins; collective thermalization, individual thermalization and individual dephasing (we ignore collective dephasing effects here at present). Now solving the master equation allows us to explore the dynamics of the overall system and we should be able to simply determine if we can reproduce the behavior observed in Fig. 2(c)—especially as we already know many of our system parameters including ω_{ns} and the fridge temperature T as well as the T_1 and T_2^* relaxation times, Our interest here will be in determining the magnetization of the double domain system which will be proportional (up to an arbitrary scaling) to the expectation value $S_z = \langle J_A^z + J_B^z \rangle$. In Fig. 3, we show the evolution of the total spin magnetization versus dwell time for an $N \sim 10^{12}$ sized nuclear spin ensemble (which is much greater than \bar{n}). With our chosen parameters it is clear that we have a number of distinct behavior arising over different time scale. Those correspond to time scale less than 1 ns (yellow shaded region), between 1–1000 ms and greater than 1 s (red shaded region). The main figure in Fig. 3 is consistent with the experimental observations of Fig. 2(c).

We need to explore these three regions in a little more detail starting with the short time regime shown in the inset for a total spin number $N = 10^{12}$. First and foremost the decay process we observe here occurs much faster than either the T_2^* or T_1 times associated with individual nuclear spins. The collective thermalization term in our master equation does reproduce such behavior giving us strong evidence of collective

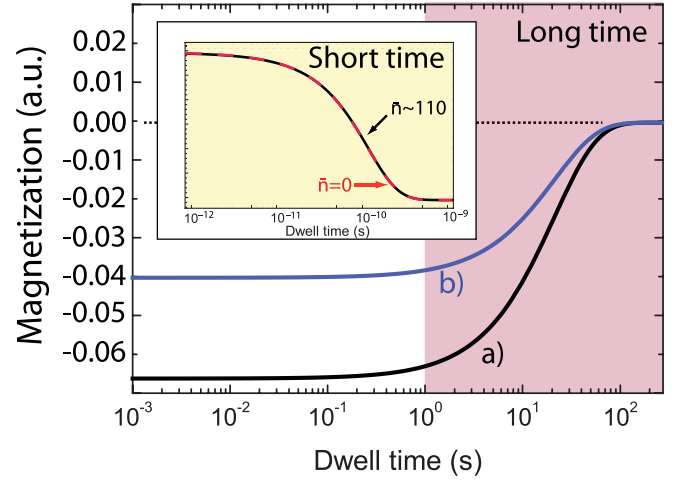


FIG. 3. Simulation of the total magnetization of the double domain nuclear spin vs the interaction (dwell) time, noting that we have an arbitrary scaling on the y axis. The results are presented for a) $N = 10^{12}$, b) $N = 6 \times 10^{12}$. Here we have used the parameters $\omega_{\text{ns}}/2\pi = 10$ MHz, $T = 50$ mK, $T_2^* \sim 1$ ms, and $T_1 \sim 40$ s. This implies that $\bar{n} \sim 110$ which is much less than N . Two distinct regions are shown in the main figure: White (red) where individual spin dephasing (thermalization) are the dominant behaviours. The yellow colored inset shows the short time behavior where collective thermalization effects dominate. Within the inset the black (red-dashed) curves correspond to thermal mean photon number $\bar{n} \sim 110$ (zero temperature $\bar{n} \sim 0$). Little difference is seen for the two \bar{n} as both are much less than N .

and coherent effects here. Next the individual dephasing of the nuclear spins with associated $T_2^* \sim 1$ ms dominates in the 1–1000 ms temporal region where it destroys all coherence within and between the nuclear spins leaving the double domain system in a separable state. Each of the nuclear spins are now acting independently of each other and so collective effects do not arise. At approximately 1 s the effect of individual nuclear spin thermalization begins and at approximately 100 s the nuclear spins reach their high temperature steady state (with a magnetization of zero). A similar behavior (blue curve in Fig. 3) occurs if N decreases but with a different degree of short time total magnetization is reached. The long time steady state is the same. Our model naturally explains the observed experimental behavior and can give us further incites into our system dynamics.

The particularly interesting temporal behavior arises in the short time regime where we observe a fast decrease in the total magnetization to a little well below zero. We only observe the resultant effect here and not its dynamics which we can not experimentally measure. We only see the result that this collective behavior has caused. Our model however can also be used to explore the short time regime in more theoretical detail. It is clear from our model (with $\bar{n} = 0$ that the rate of thermalization scales quadratically with N (rather than linear from individual spin thermalization). This is consistent with superradiance decay. Next for $\bar{n} \sim 110$, we observe a very similar quadratic short time behavior, however as $\bar{n} \rightarrow N$ we loss that quadratic behavior. In our experiment we realistically have $N > 10^{12}$ which is much greater than the $\bar{n} \sim 110$

associated with the nuclear spin operating at 50 mK. For such a large N the associated superradiant decay time is extremely fast ($<10^{-10}$ s) and hence is impossible to observe. Our observed experimental behavior however is only consistent if such collective decay had occurred.

To summarize, we have shown how collective and coherence effects arise in a double domain nuclear spin ensemble coupled to the Nambu-Goldstone boson in a GaAs semiconductor. The NG bosons long wavelength means both nuclear spin ensembles couple see the same mode. This leads to superradiant like decay event when our system is operating in the regime ($\hbar\omega_{\text{ns}} \ll k_B T$). Further it is likely that the short

time dynamics will show entanglement between the two ensembles. This will open a new paradigm in nonlinear systems where quantum only effects are present.

We thank Yusuke Hama and Shane Dooley for valuable discussions. This work was supported in part by the MEXT Grant-in-Aid for Scientific Research on Innovative Areas KAKENHI Grant No. JP15H05867 (Y.H.) and JP15H05870 (K.N.), MEXT Grant-in-Aid for Scientific Research(S) KAKENHI Grant No. JP25220601 (K.N.) and Grant-in-Aid for Scientific Research(A) KAKENHI Grant No. JP19H00662 (W.J.M. and K.N.).

-
- [1] M. A. Nielsen and I. L. Chuang, *Quantum Computation and Quantum Information* (Cambridge University Press, Cambridge, UK, 2000).
- [2] T. P. Spiller and W. J. Munro, *J. Phys.: Condens. Matter* **18**, V1 (2005).
- [3] J. P. Dowling and G. J. Milburn, *Phil. Trans. R. Soc. A* **361**, 1655 (2003).
- [4] N. Gisin, G. Ribordy, W. Tittel, and H. Zbinden, *Rev. Mod. Phys.* **74**, 145 (2002).
- [5] P. W. Shor, *SIAM J. Comput.* **26**, 1484 (1997).
- [6] R. P. Feynman, *Int. J. Theor. Phys.* **21**, 467 (1982).
- [7] C. M. Caves, *Phys. Rev. D* **26**, 1817 (1982).
- [8] V. Giovannetti, S. Lloyd, and L. Maccone, *Science* **306**, 1330 (2004).
- [9] M. Wallquist, K. Hammerer, P. Rabl, M. Lukin, and P. Zoller, *Phys. Scr. T* **137**, 014001 (2009).
- [10] Z.-L. Xiang, S. Ashhab, J. Q. You, and F. Nori, *Rev. Mod. Phys.* **85**, 623 (2013).
- [11] G. Kurizki, P. Bertet, Y. Kubo, K. Mølmer, D. Petrosyan, P. Rabl, and J. Schmiedmayer, *Proc. Natl. Acad. Sci. USA* **112**, 3866 (2015).
- [12] J. M. Raimond, M. Brune, and S. Haroche, *Rev. Mod. Phys.* **73**, 565 (2001).
- [13] H. Ritsch, P. Domokos, F. Brennecke, and T. Esslinger, *Rev. Mod. Phys.* **85**, 553 (2013).
- [14] R. Schirhagl, K. Chang, M. Loretz, and C. L. Degen, *Annu. Rev. Phys. Chem.* **65**, 83 (2014).
- [15] D. Lee, K. W. Lee, J. V. Cady, P. Ovarthaiyapong, and A. C. B. Jayich, *J. Opt.* **19**, 033001 (2017).
- [16] P. Forn-Díaz, J. J. García-Ripoll, B. Peropadre, J.-L. Orgiazzi, M. A. Yurtalan, R. Belyansky, C. M. Wilson, and A. Lupascu, *Nat. Phys.* **13**, 39 (2017).
- [17] F. Yoshihara, T. Fuse, S. Ashhab, K. Kakuyanagi, S. Saito, and K. Semba, *Nat. Phys.* **13**, 44 (2017).
- [18] F. Yoshihara, T. Fuse, Z. Ao, S. Ashhab, K. Kakuyanagi, S. Saito, T. Aoki, K. Koshino, and K. Semba, *Phys. Rev. Lett.* **120**, 183601 (2018).
- [19] D. Paget, G. Lampel, B. Sapoval, and V. I. Safarov, *Phys. Rev. B* **15**, 5780 (1977).
- [20] A. Angerer, S. Putz, D. O. Krimer, T. Astner, M. Zens, R. Glattauer, K. Streltsov, W. J. Munro, K. Nemoto, S. Rotter, J. Schmiedmayer, and J. Majer, *Sci. Adv.* **3**, e1701626 (2017).
- [21] A. Angerer, K. Streltsov, T. Astner, S. Putz, H. Sumiya, S. Onoda, J. Isoya, W. J. Munro, K. Nemoto, J. Schmiedmayer, and J. Majer, *Nat. Phys.* **14**, 1168 (2018).
- [22] R. H. Dicke, *Phys. Rev.* **93**, 99 (1954).
- [23] M. Gross and S. Haroche, *Phys. Rep.* **93**, 301 (1982).
- [24] K. Cong, Q. Zhang, Y. Wang, G. T. Noe, A. Belyanin, and J. Kono, *J. Opt. Soc. Am. B* **33**, C80 (2016).
- [25] Y. Hama, W. J. Munro, and K. Nemoto, *Phys. Rev. Lett.* **120**, 060403 (2018).
- [26] Y. Hama, E. Yukawa, W. J. Munro, and K. Nemoto, *Phys. Rev. A* **98**, 052133 (2018).
- [27] R. Hanson, L. P. Kouwenhoven, J. R. Petta, S. Tarucha, and L. M. K. Vandersypen, *Rev. Mod. Phys.* **79**, 1217 (2007).
- [28] E. M. Kessler, S. Yelin, M. D. Lukin, J. I. Cirac, and G. Giedke, *Phys. Rev. Lett.* **104**, 143601 (2010).
- [29] E. A. Chekhovich, M. N. Makhonin, A. I. Tartakovskii, A. Yacoby, H. Bluhm, K. C. Nowack, and L. M. K. Vandersypen, *Nat. Mater.* **12**, 494 (2013).
- [30] S. D. Sarma and A. Pinczuk, *Perspectives in Quantum Hall Effects* (Wiley, New York, 1997).
- [31] Z. F. Ezawa, *Quantum Hall Effects: Recent Theoretical and Experimental Developments*, 3rd ed. (World Scientific, Singapore, 2013).
- [32] M. Z. Hasan and C. L. Kane, *Rev. Mod. Phys.* **82**, 3045 (2010).
- [33] X.-L. Qi and S.-C. Zhang, *Rev. Mod. Phys.* **83**, 1057 (2011).
- [34] N. Kumada, K. Muraki, and Y. Hirayama, *Science* **313**, 329 (2006).
- [35] Y. Hirayama, G. Yusa, K. Hashimoto, N. Kumada, T. Ota, and K. Muraki, *Semicond. Sci. Technol.* **24**, 023001 (2009).
- [36] K. Hashimoto, K. Muraki, T. Saku, and Y. Hirayama, *Phys. Rev. Lett.* **88**, 176601 (2002).
- [37] N. Kumada, K. Muraki, and Y. Hirayama, *Phys. Rev. Lett.* **99**, 076805 (2007).
- [38] See Supplemental Material at <http://link.aps.org/supplemental/10.1103/PhysRevB.104.L121402> for Sec. I for device and measurement details, which includes K. Akiba, S. Kanasugi, K. Nagase, and Y. Hirayama, *Appl. Phys. Lett.* **99**, 112106 (2011).
- [39] S. Das Sarma, S. Sachdev, and L. Zheng, *Phys. Rev. Lett.* **79**, 917 (1997).
- [40] L. Brey, E. Demler, and S. Das Sarma, *Phys. Rev. Lett.* **83**, 168 (1999).
- [41] J. K. Jain, *Phys. Today* **53**(4), 39 (2000).
- [42] See Supplemental Material at <http://link.aps.org/supplemental/10.1103/PhysRevB.104.L121402> for Sec. III.
- [43] O. Stern, N. Freytag, A. Fay, W. Dietsche, J. H. Smet, K. von Klitzing, D. Schuh, and W. Wegscheider, *Phys. Rev. B* **70**, 075318 (2004).

- [44] M. H. Fauzi, S. Watanabe, and Y. Hirayama, *Appl. Phys. Lett.* **101**, 162105 (2012).
- [45] J. N. Moore, J. Hayakawa, T. Mano, T. Noda, and G. Yusa, *Phys. Rev. Lett.* **118**, 076802 (2017).
- [46] We observe a slight asymmetry between the numbers of up and down nuclear spin polarization after current pumping. The nature of this asymmetry is still an open question, however, it is likely to stem from the spatial topology of electron spin domains used to dynamically polarize the nuclear spins [45].
- [47] A. Fukuda, A. Sawada, S. Kozumi, D. Terasawa, Y. Shimoda, Z. F. Ezawa, N. Kumada, and Y. Hirayama, *Phys. Rev. B* **73**, 165304 (2006).
- [48] Y. Hama, M. H. Fauzi, K. Nemoto, Y. Hirayama, and Z. F. Ezawa, *New J. Phys.* **18**, 023027 (2016).
- [49] See Supplemental Material at <http://link.aps.org/supplemental/10.1103/PhysRevB.104.L121402> for Secs. III and IV on how to initialize and calibrate the nuclear spins.
- [50] R. K. Sundfors, *Phys. Rev.* **185**, 458 (1969).
- [51] T. Ota, G. Yusa, N. Kumada, S. Miyashita, T. Fujisawa, and Y. Hirayama, *Appl. Phys. Lett.* **91**, 193101 (2007).
- [52] M. H. Fauzi, S. Watanabe, and Y. Hirayama, *Phys. Rev. B* **90**, 235308 (2014).
- [53] H. J. Carmichael, *Statistical Methods in Quantum Optics I: Master Equations and Fokker-Planck Equations* (Springer, Berlin, 2002).